Light Shift Measurements in a Cesium Fountain without the use of Mechanical Shutters

D. G. Enzer, W. M. Klipstein, and R. L. Tjoelker

Jet Propulsion Laboratory, California Institute of Technology, Pasadena, California USA
Daphna.G.Enzer@jpl.nasa.gov

Abstract— **We present measurements confirming operation of a cesium fountain frequency standard with light shift below 10^{-15} (and with evidence suggesting it is several orders of magnitude below this level) but without the use of mechanical shutters. Suppression of the light shift is realized using a master-slave laser configuration by reducing the overall optical power delivered to the physics package as well as spoiling the injection of the slave, causing it to lase far off resonance (1-2 nm) as proposed by the authors several years ago [1]. In the absence of any mitigation, this (AC Stark) shift, due to near-resonant laser light reaching the atoms during their microwave interrogation period, is the largest shift in such frequency standards (2×10^{-11} for our fountain). Mechanical shutters provided adequate light attenuation but have been prone to failure.**

Keywords- cesium fountain, light shift, frequency standard, atomic clock, injection locked lasers

I. INTRODUCTION

Several years ago we proposed operating a Cesium fountain without mechanical laser shutters while keeping the light shift below 10^{-17} [1], [2]. In the absence of any mitigation, this (AC Stark) shift, due to near-resonant laser light reaching the atoms during their microwave interrogation period, is potentially the largest shift in such frequency standards (2×10^{-11} for our fountain). Therefore, light intensity is typically reduced during this interrogation period using acousto-optic modulators (AOMs) to rapidly deflect the majority of light away from the main path. Complete attenuation is guaranteed by the additional use of mechanical shutters. Without shutters, small amounts of leakage light through the AOM can still potentially cause shifts detrimental to the 10^{-15} level of precision of many Cesium fountains.

While effective and simple, mechanical shutters are prone to failure on a time scale of months. The simple annoyance of replacing mechanical shutters instead becomes a failure mode for clocks meant to operate in space such as the PARCS experiment (Primary Atomic Reference Clock in Space) for which this new technique was originally conceived, and also for long-term rugged operation of clocks on the ground. In addition, mechanical vibrations caused by shutters create operational difficulties in many laser systems.

In our new approach, the light shift is reduced beyond what can be achieved via simple light attenuation by additionally causing the lasers to run off resonance. In our master-slave laser configuration (Fig. 1), this is achieved using the double pass (DP) AOM between master and slave originally present for adjusting the slave laser's frequency without varying its output amplitude. If the RF power on this AOM is cut, the slave laser no longer injection locks and instead free runs. The slave is also followed by a single pass (SP) AOM for amplitude control. Cutting the RF power to the SP AOM attenuates the beam reaching the atoms, while cutting the RF power to the DP AOM further reduces the light shift by detuning the slave laser to its free-running wavelength, often nanometers away from the atomic resonance.
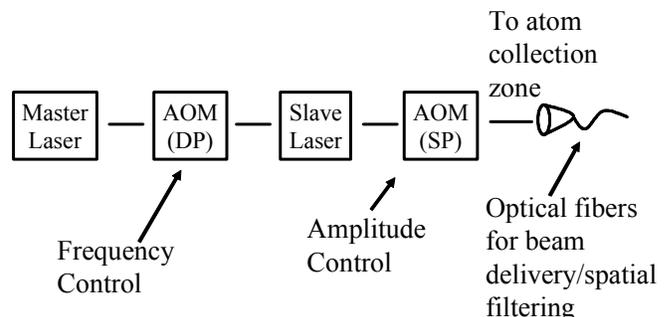
Figure 1.   A master laser beam goes through a double pass AOM and injection locks a slave laser. The slave's beam goes thorough a single pass AOM for amplitude control before being coupled to a single mode fiber for delivery to the atoms. Either the double pass or the single pass AOM can be used to attenuate the resonant light as described in the text.

Experimental verification of this concept was desired to confirm that the slave laser does not still output small amounts of light at the master laser frequency or produce a broadband spectrum of light that adds to the light shift unexpectedly.

II. APPARATUS

We tested the new light shift mitigation technique on a Cesium fountain built as a testbed for the PARCS experiment, originally slated to fly on the International Space Station. The fountain is shown in Fig. 2 and described in more detail in [3]. Distinguishing features include: magnetic shielding of the entire physics package (no magnetic trim coils in the atom collection chamber), all laser beams delivered to the physics package via optical fiber, no mechanical adjustments of optics on the fountain (everything bolts on as built), welded re-entrant windows in titanium and copper walls, and a re-entrant "spill proof" cesium source operated at room temperature. Typical Allan deviations are $(2 - 3) \times 10^{-13} \tau^{-0.5}$ down to the stability of the distributed maser local oscillator signal (near 10^{-15}).
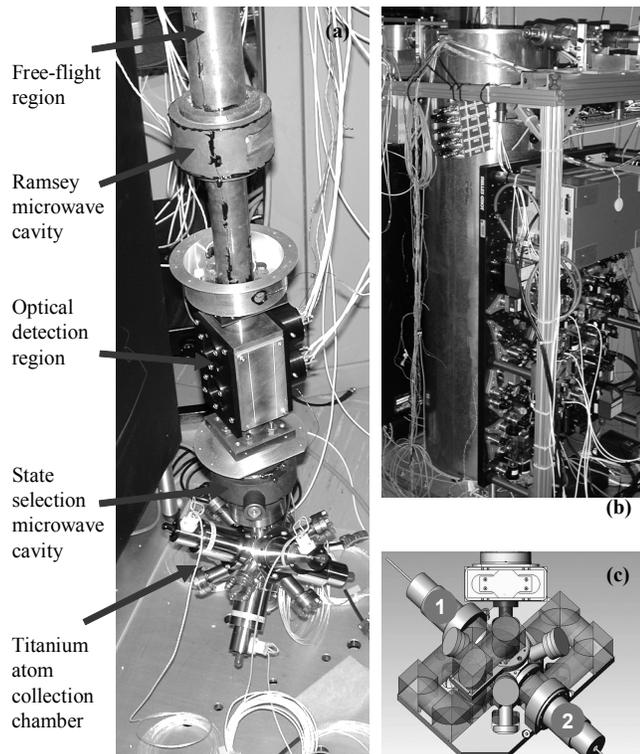
Figure 2. (a) Bottom section of Cs fountain used for these measurements shows all the crucial regions. (b) Fully assembled Cs fountain within three layers of magnetic shielding and with laser system mounted on compact frame. (c) Schematic showing that only 2 collimators are required for the recirculation technique.. After recirculation occurs via the polarizing beam-splitter cubes shown, collimator 1 provides three beams whose resultant propagation vectors point down, and collimator 2 provides three beams whose resultant propagation vectors point up.

The six orthogonal laser beams used to trap and cool atoms into a lin $\perp$ lin 3-D optical molasses (see e.g. [4], [5]) in the atom collection region are arranged in a typical 1-1-1 geometry but delivered in a nontraditional way. Fig. 2a shows the original (more traditional) way these beams had been delivered, via six independent (polarizing maintaining) fibers injecting light into six separate collimators. As described in [3], however, we later switched to a recirculation configuration shown in Fig. 2c where one fiber

is delivered for the three beams whose propagation vectors point down and one fiber for the three beams whose propagation vectors point up. This technique has the advantage of simplifying the laser system, providing more optical power throughput, and simplifying intra-beam power balancing. All data for the current paper are taken using the recirculation configuration.

III. MEASUREMENT TECHNIQUE

In order to verify that the slave laser detuning technique is effective at eliminating light shift we operate the fountain in different modes in which resonant laser light is attenuated using one of four methods: free running slaves (FR), simple attenuation of the slaves (AT), FR plus AT, or AT plus shutters. We assume the mode that uses shutters is free of light shift and therefore compare the measured clock frequency in each of the first three modes to this last mode. Note that the free running mode is achieved by cutting the RF power to the DP AOMs such as the one shown in Fig. 1, while the AT mode is achieved by cutting the RF power to the SP AOMs such as the one shown in the same figure.

To eliminate long-term drifts such as that of the local oscillator (a maser signal stable to $\sim 10^{-15}$ from 1000-10,000 seconds and distributed from a nearby building via fiber optic cable), we cycle through all four modes making all frequency comparisons within 1600 seconds. In this time we perform 100 clock frequency measurements in each mode (2 launches per frequency measurement; 1.96 s per launch). This process is then repeated, and the full data set reported here includes 334 repetitions over the course of 15 days (not all contiguous). The experimental cycle was specifically chosen to take advantage of the maser local oscillator stability and to use it as a flywheel. Note that attenuation methods other than the four above were also tested and diagnostics were performed so that the total repetition time from one set to the next was actually 2800 s, even though the frequencies of interest were all determined within 1600 s.

Frequency measurements are performed in a standard way (see for e.g. [6] and [7]). Atoms are cooled, collected and launched at 4.1 m/s in all F=4 states, and then state-selected to the F=3; m_F=0 state. Launched atoms pass through the Ramsey cavity twice, once on their way up and once on their way down with a total Ramsey time of 470 ms in between. We phase modulate the microwaves by changing their phase during the second pass to either +90° or -90° from that of the first pass and then compare the percentage of atoms coming back in the F=3 state for alternate phases. With these measurements and knowledge of the Ramsey fringe slope, we determine how close the applied microwave frequency is to the Cesium clock resonance, and monitor changes in the clock frequency due to light shift or other causes.

Fig. 3 shows a sample time-of-flight fluorescence signal as the downward going atoms pass through a 2 mm sheet of resonant, circular-polarized probe light. The detection area has two detectors with a repump beam in-between. The

upper detector (DET2) detects F=4 atoms; the lower detector (DET1) detects F=3 atoms. The number of atoms detected in a given state (proportional to area under curve in Fig. 3) is always normalized by the total number of atoms seen in both detectors. In this way we generate the normalized Ramsey fringe curve shown in Fig. 5 from the raw data shown in Fig. 4. Besides normalizing, Fig. 5 also accounts for two offsets, one of which is illustrated by the arrow in Fig. 4. The fringes do not reach zero on resonance, indicating that some portion of launched atoms are not taking part in the Ramsey transition (typically 4-5% of total atom number for DET1, F=3 atoms). This loss of contrast is suspected to be due to microwave leakage. Similar fringes collected with a 180° phase shift between microwaves on the way up versus down, reveal the offset for DET2, F=4 atoms (typically 2-3%). These offsets are characterized more in the systematics discussion.

Figure 5. Similar Ramsey fringes to those of Fig. 4, but with each point normalized to the total number of atoms participating in oscillations (i.e. offsets are removed as described in text). Inset shows the normalized central Ramsey fringe with ~1 Hz FWHM.
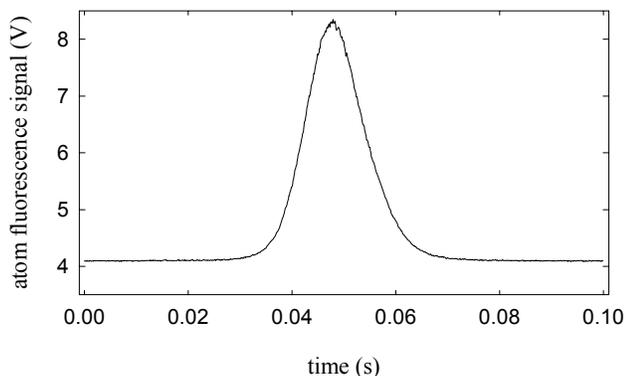
Figure 3. Time-of-flight fluorescence signal for atoms going down through detection region. Area under the curve is proportional to the number of atoms.

IV. RESULTS

Results are shown in Table I. All frequencies are relative to the presumed light-shift-free case (AT plus shutters). The full-light-shift was monitored by occasionally checking the clock frequency with all lasers left on (and injection locked) except the atom collection region's repump laser. This repump was kept off to prevent collecting atoms that would fluoresce and direct extra light up toward the interaction region. Absence of fluorescence/scattering was confirmed by measuring this full-light-shift as a function of laser detuning and verifying the expected inverse linear relationship (see (2) in next section). We also confirmed that the light shift is predominantly due to the two trapping/cooling lasers which free-run 1 and 2 nm blue of resonance. Shifts from the probe and repump beams were at least an order of magnitude smaller (tuned just off resonance to maximize the light shift).

TABLE I.   MEASURED LIGHT SHIFTS

Attenuation Configuration	Fractional Frequency Shift (relative to AT+shutters)
NO attenuation (i.e. full light shift)	-2.4×10^{-11}
free running slaves (FR)	$2.1 \pm 0.8 \times 10^{-15}$
attenuating slaves (AT)	$0.3 \pm 0.8 \times 10^{-15}$
FR plus AT	$-0.3 \pm 0.8 \times 10^{-15}$

The baseline full light shift of -2.4×10^{-11} varied at most 7% from its maximum to its minimum over the course of the 15 days. The other three lines of the table show that just free running the slave lasers (FR) gave ~10^4 reduction in light shift, just attenuating the slave lasers (AT) reduced the light shift by more than 10^4 to below our statistical uncertainty

Figure 4. Raw data showing rapidly oscillating Ramsey fringes superimposed on a broader Rabi profile. Plotted are areas under the time-of-flight fluorescence signals (Fig. 3) as a function of applied microwave frequencies. No phase change is applied between the first and second pass through the Ramsey microwave cavity. Arrow indicates that some atoms do not participate in the oscillations and thus contribute to an offset.

($\pm0.8\times10^{-15}$) and using both methods did not introduce any unexpected artifacts and therefore also reduced the light shift to our measurement limit. If the FR and AT reductions in light shift are independent, one might expect a $>10^8$ attenuation when using both, reducing the light shift to $<2\times10^{-19}$, but this is un-verifiable at this time. The error bars in the table are statistical errors on the difference frequencies reported.

The demonstrated effectiveness of this slave laser detuning technique indicates that it can be used for light shift reduction below 10^{-15}, even in fountains with much higher light scattering or with vertical beams for which the AT method alone would not be adequate.

V. COMPARISON WITH CALCULATIONS

Following the calculation presented in [1], we estimate the expected light shift for far-detuned and near-resonant light. In the dressed-state-picture, two generalized energy levels are shifted by an applied light field as shown in Fig. 6 [8], [9], where $\Omega_{eff} = \sqrt{\Omega^2 + \delta^2}$ is the effective Rabi frequency, δ is the detuning (laser frequency minus atomic frequency), Ω is the Rabi frequency,

$$\Omega^2 = C_{ge}^2 \frac{I}{I_s} \frac{\gamma^2}{2},\qquad(1)$$

I is the light intensity, I_s is the on-resonance saturation intensity, γ is the linewidth of the optical transition, and C_{ge} is the Clebsch-Gordan coefficient that describes the coupling between the atom and the light field. In this picture, for positive detuning δ, the ground state is the upper level and has a positive light shift, whereas for negative detuning, the ground state is the lower-level and has a negative light shift. The ground state is then shifted in energy by

$$\Delta E_{gs} = \frac{\hbar}{2}(\Omega_{eff} - |\delta|)\frac{\delta}{|\delta|} \approx \frac{\hbar\Omega^2}{4\delta},\qquad(2)$$

where the second expression is valid for the weak intensity regime our measurements all fall within $\Omega \ll |\delta|$.

For a given stray light laser frequency that can couple each hyperfine level to a particular excited state as in Fig. (6), the detuning (laser frequency minus atomic frequency) to each of the hyperfine levels is slightly different, leading to a differential energy shift,

$$\Delta E_{gs4} - \Delta E_{gs3} \approx -\frac{\hbar C_{ge}^2}{8}\frac{I}{I_s}\gamma^2\frac{(\delta_4 - \delta_3)}{\delta_4\delta_3}.\qquad(3)$$

Here δ_4 is the detuning to the F=4 hyperfine level, δ_3 is the detuning to the F=3 hyperfine level, and $(\delta_4 - \delta_3)/(2\pi)$ is always positive and is the clock frequency ν = 9.2GHz. This *differential* shift is what affects the clock frequency.

$$\hbar\delta \qquad \hbar\Omega_{eff} = \hbar\sqrt{\Omega^2 + \delta^2}$$
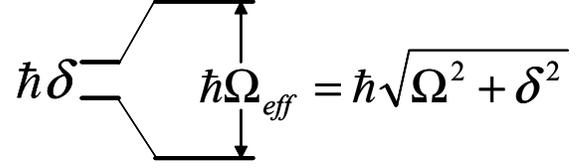
Figure 6. Two unshifted (left) and shifted (right) energy levels in the dressed-state picture. When δ is positive, the ground state is the upper level.

For far detuned light $|\delta| \gg \delta_4 - \delta_3$, where $\delta \approx \delta_4 \approx \delta_3$. The fractional clock frequency shift is then

$$\frac{\Delta\nu}{\nu} \approx -\frac{C_{ge}^2}{8}\frac{I}{I_s}\frac{\gamma^2}{\delta^2} \quad \text{(far-detuned)},\qquad(4)$$

where we have substituted the clock frequency ν for $(\delta_4 - \delta_3)/(2\pi)$. Note that the clock shift for far-detuned light is always negative.

When we do *not* allow the slave lasers to free run, the laser light is much closer to resonance with *one* of the hyperfine levels and that level's light shift then dominates the overall clock shift. In the case where the dominant light source is near resonance with F=4, $|\delta| \ll \delta_4 - \delta_3$, where $\delta \approx \delta_4$, and including spontaneous emission as in [4] or [5], (2) or (3) gives

$$\frac{\Delta\nu}{\nu} \approx \frac{C_{ge}^2}{2}\frac{I}{I_s}\frac{\delta}{(1 + (2\delta/\gamma)^2)2\pi\nu} \quad \text{(near F=4)}.\qquad(5)$$

This formula is still only valid in the weak intensity regime $\Omega \ll |\delta|$. For light near the F=3 resonance, this near-resonance clock shift has the opposite sign. Notice that the magnitude of the frequency shift for far-detuned light (4) is just the magnitude of the frequency shift for near-resonant light (5) scaled by $2\pi\nu/|\delta|$, (ignoring the spontaneous emission term in the denominator which is negligible for far-detuned light).

Finally, we can substitute parameter values from Table II to estimate the near-resonant and far-detuned light shifts assuming $I = P/(\pi r^2)$, where P is the laser power reaching the interrogation region and r is the beam-tube radius over which the light is spread. Using the light shift estimate in (5) to derive the measured full-light-shift -2.4×10^{-11}, we deduce the power reaching the interaction region to be $P = 2.6\times10^{-6}$ mW. For ~300-400 mW of recirculated light input to the atom collection region, this implies a scattering fraction of only 5-7 $\times10^{-9}$.

TABLE II. VALUES USED IN ESTIMATION OF THE LIGHT SHIFT

Parameter	Value (far-detuning)	Value (near-resonance with F=4 state)
linewidth, $\gamma/2\pi$	5 MHz	
beam-tube radius, r	0.75 cm	
saturation intensity, I_s	1.1 mW/cm^2	
average Clebsch-Gordan coefficient, C_{ge}	0.816	0.745
detuning, $\delta/2\pi$	+413 GHz (i.e. 1 nm)	−10 MHz

Taking $P = 2.6 \times 10^{-6}$ mW, (4) gives an estimate for the far-detuned light shift from the trapping/cooling lasers, i.e. the light shift in the FR mode. This calculated value of -1.7×10^{-17} is 100 times smaller than (and opposite sign to) what we actually measure, easily explained by small amounts of leakage light near-resonance. Leakage can arise if zero or first-order light from the DP AOM reaches the slave laser and causes it to lase at a near-resonant frequency, or if the free-running slave laser naturally has some output near resonance. In general, the amount of leakage could be dependent on the opto-mechanical setup, and thus future use of this technique should rely on confirming the ability of the DP AOMs to reduce the light shift several orders of magnitude in the FR mode as done here.

VI.   SYSTEMATICS

In this section we describe systematics that were checked and/or controlled including: laser intensity, temperature, collision shift/atom number, microwave power, maser jumps, and sensitivity to detector offsets.

The collision shift was measured to be $\sim -2 \times 10^{-14}$ for the number of atoms typically launched, so atom number needed to be held constant to better than 4% over a 1600 s data set to keep the collision shift below the statistical uncertainty 0.8×10^{-15}. Atom number varied with intensity of the trapping/cooling lasers, and also with room temperature (through the Cesium source pressure). Laser intensities for trapping/cooling and probe beams were all held constant using electronic servos that controlled the RF input power to the SP AOM. The room remained within a 3°C temperature range over the course of the 15 days of data. Overall, the worst-case long term drift of atom number was monitored to be only 0.6% per 1600 s set. Shot to shot variability was typically ±1-2%.

Maser local oscillator performance was tracked by comparing it to another maser. Typical drifts over a 1600 s data set were 9×10^{-17} (5×10^{-15} per day), and the worst drift over the 15 days of data was still a negligible 2×10^{-16} per 1600 s. A few much larger short-term drifts occurred, but we excluded data from these short time periods. Shifts due to the fiber frequency distribution cable were not monitored but

were previously measured and are expected to be stable over such short time periods [10].

We tested sensitivity to the two detector offsets mentioned in the Section III (one is shown in Fig. 4) which are used in calculating the percentage of atoms coming back in the F=3 versus F=4 states. We analyzed a subset of the data using different values for these input parameters to determine how sensitive the final result is to drifts. This is akin to testing our sensitivity to small drifts in Ramsey fringe contrast. Fig. 7 shows the resulting calculated frequency errors where zero error corresponds to assumed parameters for that data run. Detector offsets were monitored throughout each data run, and stayed constant to within 0.2% of total atom number per set, causing a frequency error of at most 3×10^{-16}. Drift of these offset values is due to microwave power drift discussed next where this frequency error is confirmed in a different way.
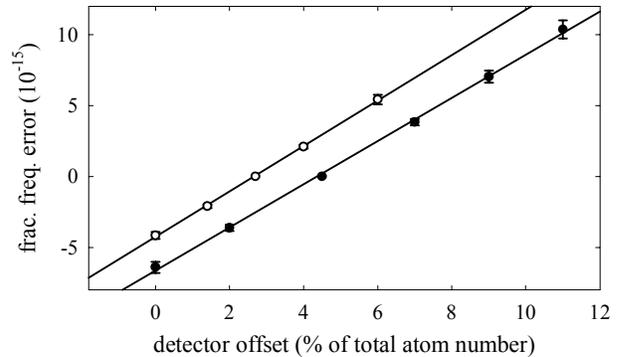
Figure 7.   When analyzing clock data, different detector offset values lead to different deduced frequencies. Fractional frequency shifts as a function of detector offset are shown for detector 1 (filled circles) and detector 2 (unfilled circles). Linear regressions (lines) give y = 1.5x - 6.6 for detector 1 and y = 1.6x - 4.3 for detector 2.

We set the microwave power as close as possible to that of a $\pi/2$ Rabi pulse. At this power (and with no phase change between the two passes) the atoms make as complete a transition as possible from F=3 to F=4 (and thus give a minimum DET1 offset). At the end of each 2800 s data set, the DET1 offset was checked and then also measured using 1 dB extra microwave power and 1 dB less. We used these measurements as diagnostics to monitor drifts in microwave power. The worst-case drift in measured DET1 offset at ±1 dB off ideal was 0.1% of total atom number per set. Fig. 8 shows measured DET1 offsets and clock shifts as a function of microwave power. From Fig. 8a, DET1 offset value has to change at least 1.6% to indicate a 0.5 dB power change when the microwave power is ±1 dB off ideal. From Fig. 8b, a 0.5 dB power change at up to 1 dB from the ideal $\pi/2$-pulse power could give as much as a 5×10^{-15} clock shift. Therefore, our worst-case DET1 value variation of 0.1% per set confirms our estimate above of a negligible 3×10^{-16} clock error. Note that this sensitivity to microwave power drift could be mitigated by steering the microwaves closer to the clock frequency. For these measurements, the microwaves

were detuned from the clock frequency by $+1.5\times10^{-13}$. We have since implemented steering.
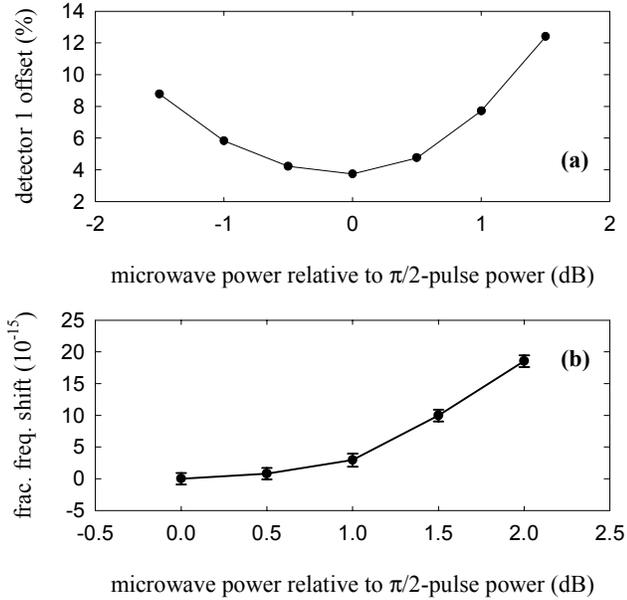
Figure 8. When the microwave power drifts from its ideal value for a $\pi/2$-pulse, changes occur to the detector offsets and to the measured clock frequency. Detector 1 offsets (a) and fractional frequency shifts (b) are shown as a function of applied microwave power. Detector 1 offset measurements are used to monitor the drift in the microwave power, as discussed in the text.

Finally, we performed other checks including reversing the order of the attenuation modes and testing other attenuation modes with shutters such as one in which the SP AOMs are only turned off briefly and then turned back on once the shutters have closed. No noticeable differences were observed. We removed occasional glitches in the data where the number of atoms detected was many standard deviations from the mean; however, we kept all other data which included 4 clock frequency measurements that were >4 standard deviations from the mean (8 are expected for 334 sets of 400 frequency measurements).

VII. CONCLUSION

We have demonstrated that it is possible to mitigate the light shift in laser cooled frequency standards without the use of mechanical shutters. Two different attenuation techniques, one using SP AOMs to attenuate the laser light (AT mode), and one using DP AOMs to detune it (FR mode), independently reduce the light shift by $>\sim 10^4$. When both techniques are used together, the light shift is confirmed to be $<10^{-15}$ and expected to be $<2\times10^{-19}$. This result should have important implications for building fountain clocks that can operate for longer periods without human intervention.

REFERENCES

[1] W. M. Klipstein and D. G. Enzer. "Mitigation of the light shift in laser cooled clocks without mechanical shutters," Proc. Freq. Contr. Symp., New Orleans, pp. 484-486, 2002.

[2] We believe the group of K. Gibble has operated a Rb fountain without shutters and with low light shift, private communication.

[3] D. G. Enzer and W. M. Klipstein. "Performance of the PARCS testbed Cesium fountain frequency standard," Proc. 2004 IEEE Int. Freq. Contr. Symp. and Exposition, Montreal, pp. 775-780, 2004.

[4] H. J. Metcalf and P. van der Staten, Laser Cooling and Trapping, New York: Springer, 1999, ch. 8.

[5] J. Dalibard and C. Cohen-Tannoudji, "Laser cooling below the doppler limit by polarization gradients: simple theoretical models," J. Opt. Soc. Am. B, vol. 6, no. 11, pp. 2023-2045, Nov. 1989.

[6] W. M. Klipstein, G. J. Dick, S. R. Jefferts, F. L. Walls "Phase modulation with independent cavity-phase control in laser cooled clocks in space," Proc. Freq. Contr. Symp., Seattle, pp. 25-32, 2001.

[7] S. R. Jefferts et al., " Accuracy evaluation of NIST-F1," Metrologia, vol. 39, pp. 321-336, 2002.

[8] C. Cohen-Tannoudji, J. Dupont-Roc, G. Grynberg, Atom-Photon Interactions, New York: Wiley, 1992, ch. 6.

[9] H. J. Metcalf and P. van der Staten, Laser Cooling and Trapping, New York: Springer, 1999, pp. 7-9.

[10] M. Calhoun, private communication.